PROCEEDINGS OF THE 9TH SSTA CONFERENCE, GDAŃSK-JURATA, POLAND,
14–16 OCTOBER 2009

Shell Structures: Theory and Applications

VOLUME 2

Editors

Wojciech Pietraszkiewicz
The Szewalski Institute of Fluid-Flow Machinery, Polish Academy of Sciences, Gdańsk, Poland

Ireneusz Kreja
Faculty of Civil and Environmental Engineering, Gdańsk University of Technology, Gdańsk, Poland

CRC Press
Taylor & Francis Group
Boca Raton London New York Leiden

CRC Press is an imprint of the
Taylor & Francis Group, an **informa** business

A BALKEMA BOOK

Shell Structures: Theory and Applications, Vol. 2 – Pietraszkiewicz & Kreja (eds)
© 2010 Taylor & Francis Group, London, ISBN 978-0-415-54883-0

Refined results on buckling of the axially compressed circular cylinder

S. Opoka & W. Pietraszkiewicz
Institute of Fluid-Flow Machinery, PASci, Gdańsk, Poland

ABSTRACT: We present extensive numerical results on bifurcation buckling analysis of the axially compressed circular cylinder. The analysis is based on the modified displacemental version of the non–linear theory of thin elastic shells developed recently by the authors. The numerical analysis of the buckling load is performed for the cylinders with eight sets of incremental work–conjugate boundary conditions analogous to those summarized in the book by Yamaki (1984), and with six sets of boundary conditions not discussed yet. The results allow us to formulate several novel important conclusions.

1 INTRODUCTION

Stability of the axially compressed thin, isotropic, elastic circular cylinder was analysed in thousands of papers, as well as summarised in several books and dozens of surveys which were briefly reviewed by Opoka & Pietraszkiewicz (2009b). In particular, Yamaki (1984) compared the buckling load curves based on Donnell's and Flügge's stability equations for a wide range of length-to-radius ratio of the cylinder and for eight sets of incremental boundary conditions, using the membrane prebuckling state. He found that with the increase in the cylinder length the buckling loads following from the Flügge stability equations took considerably smaller values than those following from the Donnell ones.

In this paper we present the extensive numerical results on bifurcation buckling of the axially compressed circular cylinder. The analysis is based on the modified version of the geometrically non-linear theory of thin, isotropic, elastic shells expressed in terms of displacements as the only independent field variables developed by Opoka & Pietraszkiewicz (2009a,b). In those papers we have formulated the modified equilibrium equations as well as the alternative work-conjugate sets of geometric and static boundary conditions compatible with a new boundary function α rational in terms of displacement derivatives. Applying this modified version of shell theory we are able to refine the results summarized by Yamaki (1984) in three main aspects:

- The two–dimensionally exact, non–linear boundary value problem (BVP) and the corresponding linearized shell buckling problem (SBP) are generated automatically by the computer programs written within the symbolic language of MATHEMATICA. Such an approach allows one to always account for those a few small terms in the SBP which may be critical for finding the correct buckling load of the axially compressed circular cylinder.
- The incremental boundary conditions of the SBP are derived by direct linearization of work-conjugate sets of the non–linear geometric and static boundary conditions about the prebuckling equilibrium state. This set allows one either to confirm the results published elsewhere, or to refine those which seem to be questionable.
- We discuss buckling loads of the compressed cylinder for eight sets of boundary conditions also investigated by Yamaki (1984). Additionally, we analyse buckling loads for six other sets of boundary conditions not discussed elsewhere.

2 DISPLACEMENT SBP FOR THE AXIALLY COMPRESSED CIRCULAR CYLINDER

The reference surface $\mathcal{M}$ of the circular cylinder with radius R, length L, and thickness h is loaded by the compressive axial force component uniformly distributed on both boundaries perpendicular to cylinder's generators. The cylindrical surface is parameterized by non-dimensional coordinates $(\phi, x = z/R)$. The independent field variables of the BVP are displacements of the reference surface. The non-dimensional incremental displacements $u(\phi, x)$, $v(\phi, x)$ and $w(\phi, x)$ denote, respectively, the axial, circumferential and radial components of the incremental displacement vector divided by R, see Fig. 1.

The modified displacemental version of the non-linear theory of thin elastic shells used here was presented in detail in the paper by Opoka & Pietraszkiewicz(2009a). In particular, formulation of the BVP for the cylinder and derivation of the corresponding SBP were generated automatically in Opoka & Pietraszkiewicz (2009b) by two packages *ShellGeom.m* and *ShellBVP.m* written within the symbolic language of MATHEMATICA.

Under the axial compressive force components $N_\nu^* = -\frac{2\rho}{\epsilon}$, the cylinder becomes shorter and is

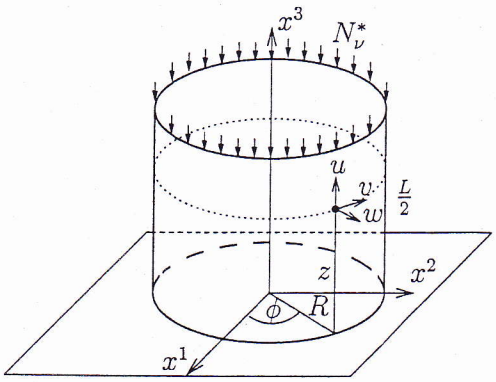

Figure 1. The parameterized upper-half of the cylindrical surface.

assumed to homogeneously expand in the radial direction. The prebuckling equilibrium solution for the cylinder can be found to be

$$u_0(\phi,x) = -2\epsilon\rho(1+3\epsilon\rho)x\,,$$
$$v_0(\phi,x) = 0\,, \tag{1}$$
$$w_0(\phi,x) = 2\epsilon\nu\rho[1+(2-\nu)\epsilon\rho]\,,$$

where ν denotes Poisson's ratio, $\epsilon^2 = h^2/[12(1-\nu^2)R^2]$, and ρ denotes the load parameter. The value $\rho = 1$ is the buckling load corresponding to the classical buckling stress $\sigma_{cl} = 2\epsilon Eh$.

The prebuckling displacements (1) are relatively small. Using the linear constitutive equations and the non-linear kinematic relations, we can show that the prebuckling solution (1) defines approximately the membrane prebuckling state with only one axial stress resultant $N_x = -\frac{2\rho}{\epsilon}$.

The displacemental SBP derived in detail in Opoka & Pietraszkiewicz (2009b) consists of three homogeneous linear PDEs with constant coefficients with regard to the incremental displacements u, v, w

$$\begin{aligned}
&A_1 w^{\cdot\cdot\cdot} + A_2 w^{\prime\prime\cdot} + A_3 u^{\prime\cdot} + A_4 v^{\prime\prime} + A_5 v^{\cdot\cdot} + A_6 w^{\cdot} = 0,\\
&B_1(w^{\prime\cdot\cdot} + \nu w^{\prime\prime\prime}) + B_2 u^{\prime\prime} + B_3 u^{\cdot\cdot} + B_4[(1+\nu)v^{\prime\cdot} + 2\nu w^{\prime}] = 0,\\
&C_1(w^{\prime\prime\prime\prime} + 2w^{\prime\prime\cdot\cdot} + w^{\cdot\cdot\cdot\cdot}) + C_2(u^{\prime\cdot\cdot} + \nu u^{\prime\prime\prime}) + C_3 v^{\prime\prime\cdot}\\
&+ C_4 v^{\cdot\cdot\cdot} + C_5 w^{\prime\prime} + C_6 w^{\cdot\cdot} + C_7 u^{\prime} + C_8 v^{\cdot} + C_9 w = 0,
\end{aligned} \tag{2}$$

and four homogeneous work–conjugate boundary conditions defined at $x = \pm l = \pm\frac{L}{2R}$

$$\begin{aligned}
&d_1 \equiv D_1 w^{\prime\prime} + D_2 u^{\prime} + D_3(v^{\cdot} + w) = 0 \ \text{ or } u = 0,\\
&d_2 \equiv E_1 w^{\prime\cdot} + E_2 u^{\cdot} + E_3 v^{\prime} = 0 \ \text{ or } v = 0,\\
&d_3 \equiv F_1[w^{\prime\prime\prime} + (2-\nu)w^{\prime\cdot\cdot}] + F_2(u^{\cdot\cdot} + \nu u^{\prime\prime})\\
&\quad + F_3 v^{\prime\cdot} + F_4 w^{\prime} = 0 \ \text{ or } w = 0,\\
&d_4 \equiv G_1(w^{\prime\prime} + \nu w^{\cdot\cdot}) + G_2 v^{\cdot} + G_3 u^{\prime} + G_4 w = 0 \ \text{ or } w^{\prime} = 0,
\end{aligned} \tag{3}$$

where $\frac{\partial()}{\partial x} = ()'$, $\frac{\partial()}{\partial\phi} = ()^{\cdot}$. The coefficients appearing in (1) and (2) are given in Opoka & Pietraszkiewicz (2009b).

Table 1. Nomenclature for different sets of clamped and simply supported boundary conditions.

C–family and S–family				
C1(S1):	$u=0$	$v=0$	$w=0$	$w'=0(d_4=0)$
C2(S2):	$d_1=0$	$v=0$	$w=0$	$w'=0(d_4=0)$
C3(S3):	$u=0$	$d_2=0$	$w=0$	$w'=0(d_4=0)$
C4(S4):	$d_1=0$	$d_2=0$	$w=0$	$w'=0(d_4=0)$
C5(S5):	$u=0$	$v=0$	$d_3=0$	$w'=0(d_4=0)$
C6(S6):	$d_1=0$	$v=0$	$d_3=0$	$w'=0(d_4=0)$
C7(S7):	$u=0$	$d_2=0$	$d_3=0$	$w'=0(d_4=0)$
C8(S8):	$d_1=0$	$d_2=0$	$d_3=0$	$w'=0(d_4=0)$

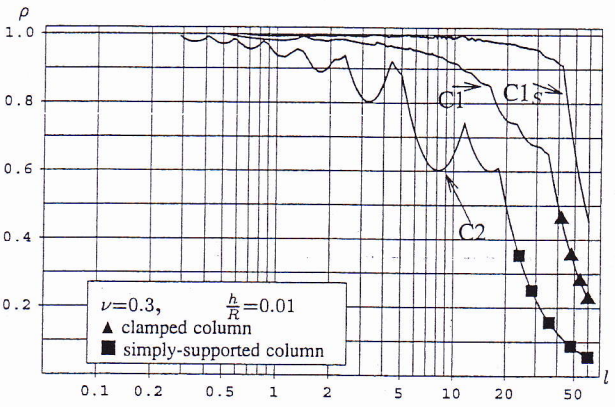

Figure 2. The buckling load of axially compressed perfect cylinder for boundary conditions C1 and C2.

Numerical results given here have been calculated for different sets of boundary conditions (3) defined in Table 1. In particular, in our nomenclature the classical simply supported and clamped boundary conditions are denoted, respectively, as S2 and C1.

3 NUMERICAL RESULTS

The solution method based on expanding displacements into Fourier series is used to generate numerical results for SBP (2) and (3). The method has been described in detail in Opoka & Pietraszkiewicz (2009b).

The numerical results indicating buckling load curves for the perfect, axially compressed cylinder with different sets of boundary conditions (see Table 1) are given in Figures 2–5. The value $\rho = 1$ corresponds to the classical value of the buckling load, and the results are positioned with respect to the horizontal, logarithmic axis of the non–dimensional cylinder length $l = \frac{L}{2R}$.

Generally, the results for fourteen types of boundary conditions (Figs. 2–5) can be divided into three groups. For the boundary conditions S1, C1, C3, C5 the buckling load takes generally high values which practically coincide when $l \in (0.7, 60)$. For S2, C2, C4, C6, C7 boundary conditions the buckling load takes intermediate values and the curves are choppy. The results for this group again practically coincide

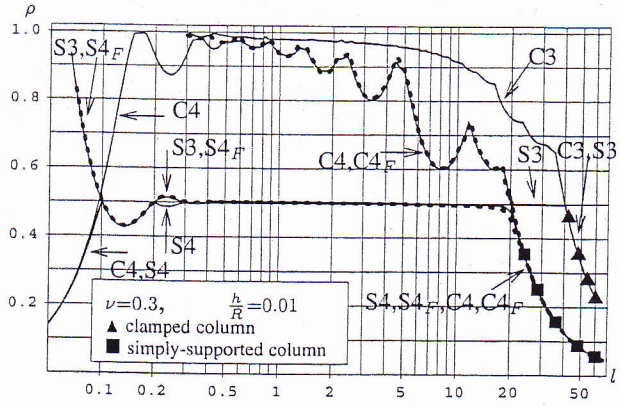

Figure 3. The buckling load of axially compressed perfect cylinder for boundary conditions S3, S4, C3 and C4.

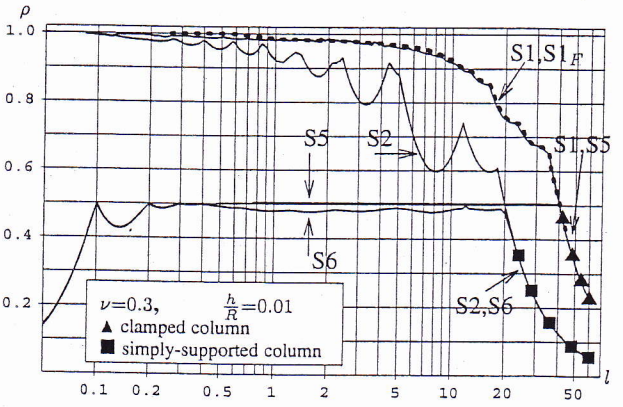

Figure 4. The buckling load of axially compressed perfect cylinder for boundary conditions S1, S2, S5 and S6.

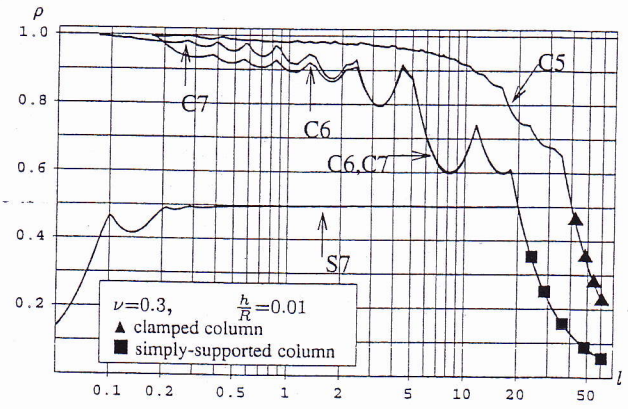

Figure 5. The buckling load of axially compressed perfect cylinder for boundary conditions C5, C6, C7 and S7.

when $l \in (2.5, 60)$. For the boundary conditions S3, S4, S5, S6, S7 the buckling load ρ assumes about one half of the classical value for intermediate cylinder lengths and the results practically coincide only when $l \in (0.1, 20)$.

The numerical results obtained using the complete SBP (C1 curve) and the simplified one, in which terms of the order of error introduced by the constitutive equations were omitted ($C1_S$ curve), are shown in Figure 2. In the intermediate length range, differences between the results are small, but with the increase of the cylinder length the simplified stability equations lead to more and more overestimated results. Hence, for the boundary conditions C1 some supposedly small terms are, in fact, important and cannot be omitted for long cylinders.

Our results have been compared with eight similar ones available in Yamaki (1984) based on the Flügge stability theory, which are represented by dotted curves in Figures 4 and 5.

For the boundary conditions C1, C2, C3, S1, S2 and S3 our results practically coincide or are slightly lower than those of Yamaki in the range of intermediate and long cylinder lengths. Thus, the Yamaki results for these cases are not shown in Figures 4 and 5, except for S1 case in Figure 4 given as an example. Because of good overall agreement between the corresponding curves, the Flügge stability equations with his boundary conditions could be preferred in applications as the simpler ones.

However, for short cylinders with boundary conditions S4 and C4 (Fig. 3) the corresponding curves in Yamaki (1984) increase with decrease in the cylinder length and exceed $\rho = 1$. But our results show that the resistance to buckling decreases in that range. This solution behaviour for the boundary conditions S4 was revealed already by Simmonds & Danielson (1970), who proved it for short cylinders using the ring–beam theory and cited the similar result noted by Koiter (1967). Our stability analysis suggests that such a behaviour follows from using in our analysis the correct, integrable forms of the geometric and associated work–conjugate static boundary conditions.

The exchange of the geometric boundary constraint $u = 0$ for the static work–conjugate boundary condition $d_1 = 0$ causes the following transition between types of boundary conditions: C1→C2, C3→C4, C5→C6, S1→S2, S3→S4 and S5→S6, see Table 1. Generally, this exchange causes that ρ_{crit} takes smaller values and within the intermediate lengths differences between the corresponding results increase as the length increases, the maximal difference being about 20%.

The exchange of boundary constraint $v = 0$ ($w = 0$) for the static work–conjugate boundary condition $d_2 = 0$ ($d_3 = 0$) leading to transitions C1→C3, C2→C4, S5→S7 (C1→C5, C2→C6, S3→S7) causes no effect within the intermediate cylinder lengths. In the transition C5→C7 (C3→C7 for $w = 0$) we have the same behaviour as in the transition C1→C2 described above. In the transitions S1→S3 and S2→S4 (S1→S5 and S2→S6 for $w = 0$), ρ_{crit} falls down to about one half of the classical value in the large range of cylinder's lengths. In cases S1→S3 and S2→S4 this phenomenon was noticed already by Hoff & Rehfield (1965) and Almroth (1966).

The exchange of the constraint $w' = 0$ for $d_4 = 0$ causes the transition from the clamped to the corresponding simply supported boundary conditions. Essentially the same results are obtained for transitions between the boundary conditions C1→S1 and C2→S2. But for the remaining ones Ci→Si,

i = 3, .., 7, ρ_{crit} falls down again to about one half of the classical value.

The buckling load for the axially compressed Euler column with simply-supported (clamped) boundaries is defined in our terms as $\rho = \frac{\pi^2}{16l^2\epsilon}$ ($\rho = \frac{\pi^2}{4l^2\epsilon}$), and its probed values are denoted in Figures 2–5 by black squares (black triangles). The axially compressed circular cylinder with the length parameter $l > 20$ and boundary conditions C2, S2, C4, S4, C6, S6, C7, S7 looses its global stability as the simply-supported Euler column, while the axially compressed very long cylinder ($l > 40$) with C1, S1, C3, S3, C5, S5 boundary conditions behaves itself as the clamped Euler column. Comparing definitions of the boundary conditions given in Table 1, the long axially loaded cylinder behaves as an axially loaded clamped column if its boundaries are constrained as $u = v = 0$ or $u = w = 0$. In the remaining cases the long axially loaded cylinder behaves as an axially loaded simply supported column. Therefore, the condition $u = 0$ indicating that the global rotation of the shell edge as a whole is not allowed, is necessary but not sufficient for the long axially loaded cylinder to behave as an axially loaded clamped column.

4 CONCLUSIONS

The numerical results allow us to formulate the following conclusions:

- If terms of the order of error introduced by the constitutive equations are omitted, this elimination leads to elimination of some supposedly small terms from the corresponding SBP. For long cylinders this results in overestimated buckling loads.
- Using the simplified kinematic relations causes the buckling load to be overestimated as well, especially for long cylinders.
- The results obtained from our complete SBP coincide in most cases with the available results following from the Flügge stability equations. However, the entirely different asymptotic behaviour has appeared for S4 and C4 boundary conditions when the length of the short cylinder is decreasing. We explain this behaviour by completeness of the work–conjugate boundary conditions used in our analysis.
- Besides the well-known case of relaxing the boundary condition $v = 0$ (transitions S1→S3 and S2→S4), which causes the buckling load to fall down to about one half of the classical value, we have also discovered that relaxing boundary conditions $w = 0$ (transitions S1→S5 and S2→S6) and $w' = 0$ (transitions Ci→Si, i = 3, .., 7) also leads to similar effects.
- The wider scatter of numerical results for simply supported cylinders, contrary to the corresponding small scatter for clamped cylinders, suggests that the buckling load is very sensitive to accurate modelling of the rotations allowed at the boundary. This seems to be one of the major reasons of discrepancy between theoretical and experimental buckling loads of the axially compressed circular cylinder.

REFERENCES

Almroth, B. O. 1966. Influence of edge conditions on the stability of axially compressed cylindrical shells. *AIAA Journal* 4(1): 134–140.

Hoff, N. J. & Rehfield, L. W. 1965. Buckling of axially compressed circular cylindrical shells at stresses smaller than the classical critical value. *Journal of Applied Mechanics* 32: 542–546.

Koiter, W. T. 1967. General equations of elastic stability for thin shells, Appendix: The danger of omitting (supposedly) small buckling terms. In *Proceedings of a Symposium on the Theory of Shells to Honor L. H. Donnell* 225–227. University of Houston.

Opoka, S. & Pietraszkiewicz, W. 2009a. On modified displacement version of the non-linear theory of thin shells. *International Journal of Solids and Structures* 46(17): 3103–3110.

Opoka, S. & Pietraszkiewicz, W. 2009b. On refined analysis of bifurcation buckling for the axially compressed circular cylinder. *International Journal of Solids and Structures* 46(17): 3111–3123.

Simmonds, J. G. & Danielson, D. A. 1970. New results for the buckling loads of axially compressed cylindrical shells subject to relaxed boundary conditions. *Journal of Applied Mechanics* 37(1): 93–100.

Yamaki, N. 1984. *Elastic Stability of Circular Cylindrical Shells*. Amsterdam: Elsevier.